Chapter 21
Luminescence and Photoconductivity

21.1 Classification of Luminescence Processes

Luminescence denotes the emission of radiation by a solid in excess of the amount emitted in thermal equilibrium and can be considered as a process inverse to the absorption of radiation. Since luminescence is basically a non-equilibrium phenomena, it requires excitation by light, electron beams, current injection, etc., which generally act to create excess electrons, holes, or both. For example, the effects of electron–hole recombination give rise to **recombination radiation** or luminescence.

One classification of luminescent processes is based on the source of the excitation energy. The most important excitation sources are

1. **photoluminescence** by optical radiation,
2. **electroluminescence** by electric fields or currents,
3. **cathodoluminescence** by electron beams (or cathode rays),
4. **radioluminescence** by other energetic particles or high energy radiation sources.

A second classification of luminescent processes pertains to the time that the light is emitted relative to the initial excitation. If the emission is fast ($\leq 10^{-8}$ s is a typical lifetime for an atomic excited state), then the process is **fluorescent**. The emission from most photoconductors is of the fluorescent variety. For some materials, the emission process is slow and can last for minutes or hours. These materials are **phosphorescent** and are called **phosphors**, and is governed by the time it takes for the carriers in the excited state to reach equilibrium. In some cases there is an excited state that is well defined, so that the occupation of the excited state has a lifetime. While the electron remains in the excited state we call the excited state an excitonic state subject to the Pauli exclusion principle. If two excitons are then excited for the same atom, a biexciton is formed where the two electrons have spin up and spin down, filling that state.

Let us now consider luminescent processes of the fluorescent type with fast emission times. The electronic transitions which follow the excitation and which result in luminescent emission are generally the same for the four types of excitations

© Springer-Verlag GmbH Germany, DE 2018

M. Dresselhaus et al., *Solid State Properties*, Graduate Texts in Physics,
https://doi.org/10.1007/978-3-662-55922-2_21

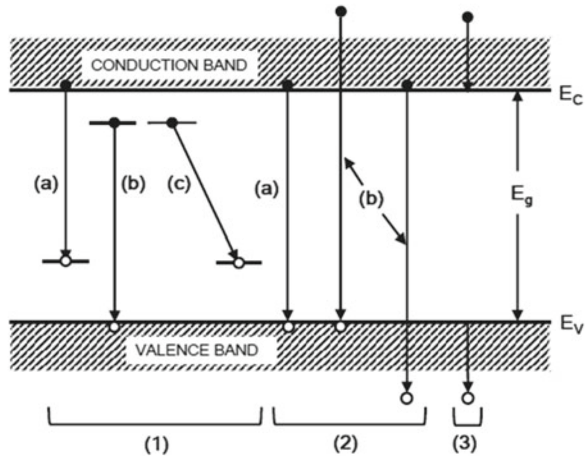

Fig. 21.1 Basic transitions in a semiconductor for stimulating the luminescent process. After H.F. Ivey, *IEEE J.Q.E.* **2**, 713 (1966). • = electrons: ○ = holes

mentioned above. Figure 21.1 shows a schematic diagram of the basic transitions in a semiconductor that are effective in exciting a luminescent process. These excitations may be classified as follows:

1. Transitions involving chemical impurities or physical defects (such as lattice vacancies):
    a. conduction band to acceptor state recombination.
    b. available electron in a donor level site makes resonant transition to a vacant conduction band state.
    c. donor to acceptor transition resulting in pair emission.
2. Interband transitions:
    a. intrinsic or edge emission, corresponding very closely in energy to the band gap, though phonons and/or excitons may also be involved.
    b. higher energy emission involving energetic or "hot" carriers, sometimes related to **avalanche** emission, where "hot" carriers refers to highly energetic carriers well above the thermal equilibrium levels.
3. Intraband transitions involving "hot" carriers, sometimes called deceleration emission.

It should be pointed out that the various transitions mentioned above do not all occur in the same material or under the same conditions. Nor are all electronic transitions radiative. Phonon emission provides a non-radiative mechanism for the relaxation of an excited state in a solid to the lowest equilibrium ground state. An efficient luminescent material is one in which radiative transitions predominate over non-radiative transitions.

When electron-hole pairs are generated by external excitations, radiative transitions resulting from the hole-electron recombination may occur. The radiative

transitions in which the sum of electron and photon wavevectors is conserved are called direct transitions as opposed to indirect transitions which involve additional available scattering agents, such as phonons.

21.2 Emission and Absorption

For a given material the emission probability will depend on the photon energy and on the temperature. The emission rate $R_{vc}(\omega)$ for the transition from the conduction band (c) to the valence band (v) is related to the absorption rate $P_{vc}(\omega)$ by the relation

$$R_{cv}(\omega) = P_{vc}(\omega)\rho(\omega) \tag{21.1}$$

where $\rho(\omega)$ is the Planck distribution function at temperature T

$$\rho(\omega) = \frac{2}{\pi}\frac{\omega^2 n_r^3}{c^3[\exp(\hbar\omega/k_B T) - 1]}, \tag{21.2}$$

and the absorption rate is given by

$$P_{vc}(\omega) = \frac{\alpha(\omega)c}{n_r}, \tag{21.3}$$

where $\alpha(\omega)$ is the frequency-dependent absorption coefficient and n_r is the index of refraction. The frequency and temperature dependence of the emission rate is then given by

$$R_{cv}(\omega) = \frac{2}{\pi}\frac{\omega^2 n_r^2 \alpha(\omega)}{c^2[\exp(\hbar\omega/k_B T) - 1]}. \tag{21.4}$$

Basically, $R_{cv}(\omega)$ shows high emission at frequencies where the absorption is large, so that emission spectroscopy can be used as a technique to study various aspects of the electronic band structure.

The luminescence process involves 3 separate steps:

1. Excitation: the electron-hole (e–h) pairs are excited by an external energy source to an excited state.
2. Thermalization: the excited electron-hole pairs relax to their quasi-thermal equilibrium distributions.
3. Recombination: the thermalized electron-hole pairs recombine radiatively to produce light emission.

We now give some examples of luminescence spectra. The big picture is shown in Fig. 21.2, where luminescence spectra for InSb are presented showing several typical features. The highest energy feature in this figure is connected with luminescence from the conduction band to the valence band (the band-to-band process) at 0.234 eV,

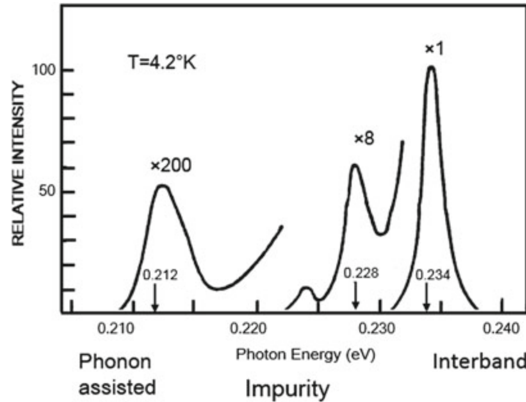

Fig. 21.2 Luminescence emission spectrum in an n-type InSb crystal with an electron concentration of $5 \times 10^{13}\,\mathrm{cm}^{-3}$. The peak at 0.234 eV is due to interband recombinative emission, and the peak at 0.228 eV is due to an impurity state below the band edge. The peak at 0.212 eV (multiplied by 200) is due to phonon-assisted band-to-band transitions. (A. Mooradian and H.Y. Fan, *Phys. Rev.*, **148**, 873 (1966).)

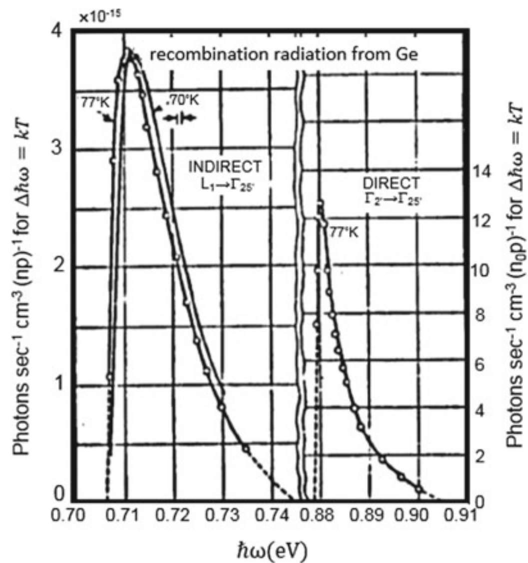

Fig. 21.3 Direct and indirect intrinsic radiation recombination in Ge. The 70 K spectrum is experimental and is in the energy range appropriate for indirect transitions assisted by longitudinal acoustic (LA) phonons. The open circles are calculated from experimental absorption data for both types of transitions. The free carrier densities at the direct and indirect conduction band minima and at the valence band maximum are denoted by n_0, n, and p, respectively

from the conduction band to an acceptor impurity level at 0.228 eV, and luminescence that is phonon assisted at 0.212 eV involving phonon absorption, so that the emitted photon has a lower energy than the excitation energy.

For intrinsic or band-to-band transitions, the peak intensity occurs near the energy gap and the width of the spectral line (at the half value of the peak intensity) is proportional to the thermal broadening energy $k_B T$. For extrinsic transitions, the peak

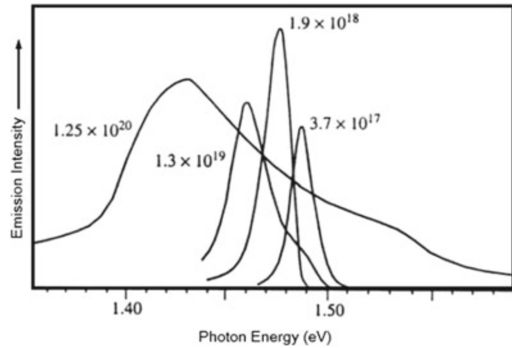

Fig. 21.4 Electroluminescence intensity of p-type (Zn-doped) GaAs at 4.2 K is shown for four different dopant concentrations, varying over 3 orders of magnitude in units of cm^{-3}. Note the increasing broadening and downshift of the emission peak with increasing dopant concentration

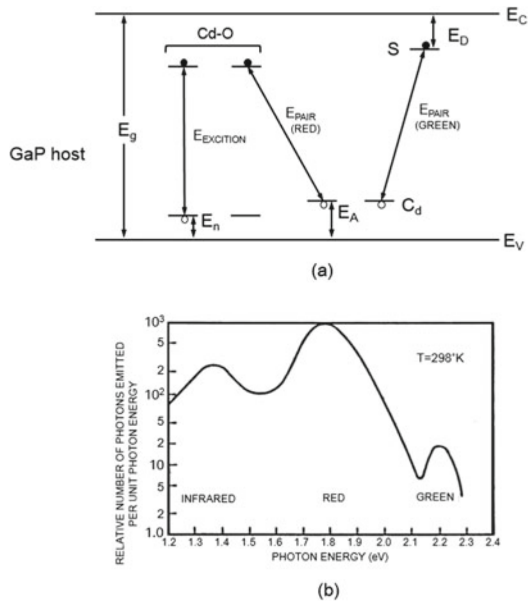

Fig. 21.5 Energy level diagram for a Cd-doped GaP $p-n$ junction where Cd-O denotes a cadmium-oxygen complex. Transitions between the exciton level of the Cd-O complex to the acceptor level of Cd give rise to red light emission. Transitions between the donor level (S) and acceptor level (Cd) give rise to the green light emission. **b** Measured emission spectrum from a GaP diode in which the color associated with the various luminescent peaks are shown ranging from infrared to red and green in the visible range. (After M. Gershenzon, Bell, *Sys. Tech. J.*, **45**, 1599, (1966).)

emission intensity occurs near the transition energy, but the broadening is greater than for the intrinsic band-to-band emission shown in Fig. 21.3 for both indirect and direct bandgap emission.

An example of a luminescence spectrum from a free to a bound state is presented in Fig. 21.4 where the electroluminescence is shown for p-type GaAs for various Zn dopant concentrations, given in units of cm^{-3}. As the impurity concentration increases, the luminescence emission becomes increasingly broad because of the perturbation to the crystal lattice introduced by the site-to-site potential variation in the basic periodicity of the lattice. Notice both the line broadening and increasing lineshape asymmetry at high dopant levels.

An example of donor-acceptor pair transitions is shown in Fig. 21.5 for GaP showing the exciton emission peak and structure associated with donor-acceptor pair emission. For donor-acceptor pair emission the energy of the emitted photon

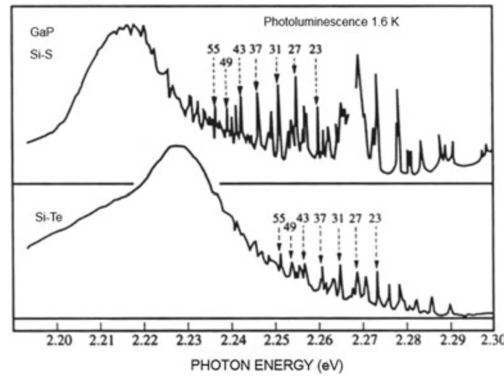

Fig. 21.6 Donor-acceptor pair (DAP) recombination spectra in GaP containing S-Si and Te-Si donor-acceptor pairs measured at low temperature (1.6 K). The integers above the discrete peaks are the shell numbers of the pairs which have been identified by comparison with theoretical predictions, for the case where each impurity is on the same sublattice (i.e., both are on the Ga or on the P sublattices). When the impurities are on different sublattices, the donor-acceptor pair recombination spectra become even more complex than what is shown in this figure

is $\hbar\omega = E_g - E_A - E_D + e^2/(\varepsilon R)$, where ε is the static dielectric constant and R is the spatial distance between the donor and acceptor impurities that constitute the electron-hole pair emission involved in the electron-hole recombination process. Because of the large number of possible sites for the donor and acceptor impurities, a very rich spectrum can be observed in the donor-acceptor pair emission, as shown in Fig. 21.6 for low temperature measurements on the wide gap semiconductor GaP.

The general problem of luminescence is not only to determine the luminescent mechanisms and the emission spectra, as discussed above, but also to determine the **luminescent efficiency**. For a given input excitation energy, the radiative recombination process is in direct competition with the non-radiative processes. Luminescent efficiency is defined as the ratio of the energy associated with the radiative process to the total input energy.

Among the fastest emission luminescent processes, electroluminescence, or excitation by an electric field or electric current, has been one of the most widely utilized for device applications. Electroluminescence is excited in a variety of ways including intrinsic, injection, avalanche, and tunneling processes, as summarized below.

1. **Intrinsic process**. When a powder of a semiconductor (e.g., ZnS) is embedded in a dielectric (plastic or glass) material, and exposed to an alternating electric field (usually chosen to be at audio frequencies), electroluminescence may occur. Generally the efficiency is low ($\sim$1%) and such materials are used primarily in display devices. The mechanism is mainly due to impact ionization by accelerated electrons and/or field emission of electrons from trapping centers.
2. **Injection process**. Under forward-bias conditions, the injection of minority carriers in a $p - n$ junction can give rise to radiative recombination. The energy level band diagram for a Cd-doped GaP $p - n$ junction is shown in Fig. 21.5.

Several different transitions for electron-hole recombination are indicated. The relative intensity of the red and the green bands can be varied by varying the impurity concentrations in the sample preparation. The red-light emission from GaP $p - n$ junctions (i.e. GaP light-emitting-diodes (LEDs)) was one of the first systems with sufficiently high efficiency to be utilized in practical applications. At a later time, high brightness, high efficiency LEDs became available throughout the IR, visible, and UV wavelength ranges, and LED technology has become a very common electronic commercial product.

3. **Avalanche process**. When a $p - n$ junction or a metal semiconductor contact is reverse-biased into an avalanche breakdown for an LED process, the electron-hole pairs generated by impact ionization may result in emission of either interband (avalanche emission) or intraband (deceleration emission) transitions, respectively.
4. **Tunneling process**. Electroluminescence can also result from tunneling into forward-biased and reverse-biased junctions. In addition, light emission can occur in reverse-biased metal-semiconductor contacts. (see M.H.P. Pfeiffer, et al. *Optics Express*, **19**, A1184–A1189, (2011).)

Fast emission luminescence also is of importance to semiconducting lasers. Luminescence is generally observed as an **incoherence** emission process in contrast with laser action, which involves the **coherent** emission of radiation in executing a radiative transition. The coherence is usually enhanced by polishing the sample faces to form an optical cavity. Examples of solid state lasers are the ruby laser and the common direct gap semiconductor lasers. Optical and electrical pumping are the most common methods of exciting laser action in solid state lasers. (see X.F. Huang et al. 2003)

Finally, we conclude the discussion of electroluminescence in semiconductors with a short discussion of slow emission luminescence, i.e. phosphorescence. Phosphorescent materials exhibit afterglow effects and are consequently important in various optical display devices. These phosphors often do not exhibit large photoconductivities. That is to say, although the electrons that were produced survive for a long time, they are bound to particular defect centers and do not readily carry charge through the crystal.

In Fig. 21.7 we show an example of how a phosphor works in an alkali halide, such as KCl with a small amount of Tl (thallium) impurities. The thallium defects act as recombination centers. If these recombination centers are very efficient at producing recombination radiation they are called **activators**; Tl doping of KCl acts as an activator. In this system, the excitation occurs at a higher energy than the emission, and therefore the excitation process is considered as an up-conversion process.

The **Franck–Condon principle** states that the atoms in the solid do not change their internuclear separations during an actual electronic transition. We now explain how emitted light is downshifted in frequency relative to the frequency of the exciting light. The Tl^+ ion in the ground or unexcited state occupies some configuration close to the symmetric center of a K^+ ion which the Tl^+ ion might be replacing. When excited, the Tl^+ ion finds a lower energy state in a lower symmetry position near one

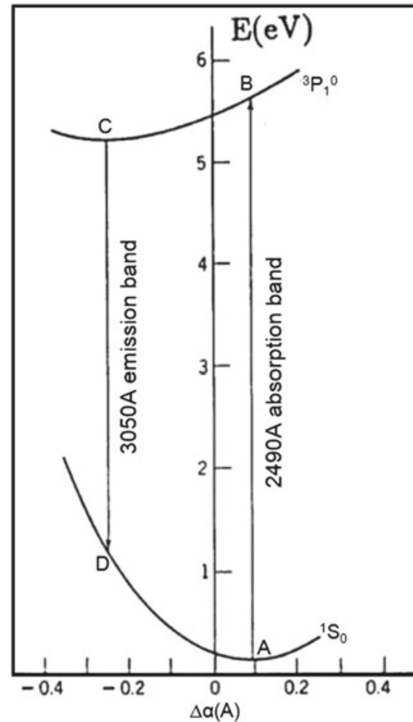

Fig. 21.7 Schematic diagram of the phosphorescence process of the thallium$^+$ activation process in KCl. The emission is downshifted from the absorption. This is an illustration of the Franck–Condon principle

of the Cl^- ions as shown schematically on the top of Fig. 21.7. The absorption is made from the ground state energy (point A in Fig. 21.7) to an excited state (point B) with the same configuration in a direct transition. Phonon interactions then will bring the electron to the equilibrium position C. Achievement of equilibrium ($B \rightarrow C$) will take a longer time than the electronic transitions ($A \rightarrow B$). Emission from $C \rightarrow D$ again occurs in accordance with the Franck–Condon principle and the readjustment to the equilibrium configuration A proceeds by phonon processes.

Photon emission is one of the main techniques for studying impurity and defect levels in semiconductors. It is an important technique also for studying new materials such as organic systems. (see Adachi et al. 2001)

One luminescent technique that has become very popular is luminescence excitation spectroscopy because of the wide variety of information that can be obtained. According to this technique the emission at a particular energy is monitored as the excitation energy is varied. This technique has become very popular for low dimensional materials systems or for very thin epitaxial layers on an opaque substrate, thereby providing much more sensitivity than absorption spectra or photoluminescence spectra offer.

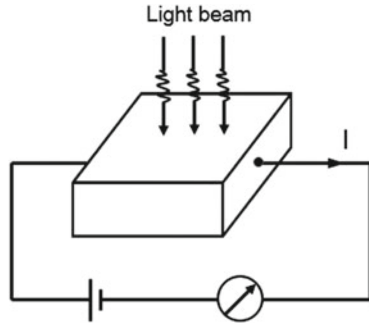

Fig. 21.8 Schematic diagram of the experimental arrangement for measuring the photoconductivity, showing a light beam incident on a sample. (see Li et al. 2014)

21.3 Photoconductivity

Photoconductivity is observed when light is incident on a poorly conducting material, (e.g., an insulator or semiconductor), and the photon energy is sufficiently high to excite an electron from an occupied valence band state to an unoccupied conduction band state. In such interband transitions, both the electron and hole will contribute to the electrical conductivity if a voltage is applied across the sample, as shown in the schematic experimental arrangement in Fig. 21.8. Since the threshold for photoconduction occurs at $\hbar\omega = E_g$, measurement of the photoconductivity can be used to determine the band gap for non-conducting materials. Photoconductivity is often the concept used for the design of practical optical detectors.

$$\Psi_{2D}(x, y) = e^{ik_x x}\phi(y) \tag{21.5}$$

The photoconduction process increases the electrical conductivity $\Delta\sigma$ due to the increase in the density of electrons (Δn) and holes (Δp) resulting from photoexcitation:

$$\frac{\Delta\sigma}{\sigma} = \frac{\Delta n\mu_n + \Delta p\mu_p}{n\mu_n + p\mu_p} \tag{21.6}$$

in which $\mu_n + \mu_p$ are respectively, the electron and hole mobilities. Since the carriers are generated in pairs in the photo-excitation process $\Delta n = \Delta p$. In preparing materials for applications as photoconductors, it is desirable to have a high mobility material with a low intrinsic carrier concentration, and long electron–hole recombination times to maximize the photo-excited carrier density concentration. Cadmium sulfide is an example of a good photoconductive material. In CdS, it is possible to change the conductivity by ∼**10 orders of magnitude** through carrier generation by light. These large changes in electrical conductivity can be utilized in a variety of device applications, such as light meters, photo-detectors, "electric eye" control applications, optically activated switches, and for information storage.

To measure the photo-currents, photo-excited carriers are collected at the external electrodes. In the steady state, free carriers are continually created by the incident light. At the same time, the excited free carriers annihilate each other through electron-hole recombination. To produce a large photocurrent, it is desirable to have a *long* free carrier *lifetime* τ' or a slow recombination time. If G is the rate of generation of electrons per unit volume due to photo-excitation, then the photo-excited electron density in the steady state will be given by

$$\Delta n = G\tau'. \tag{21.7}$$

The generation rate G will in turn be proportional to the photon flux incident on the photoconductor. Whereas slow recombination rates are essential to the operation of photoconductors, rapid recombination rates are necessary for luminescent materials.

In the recombination process, an electron and hole annihilate each other, emitting a photon in a radiative process. In real materials, the recombination process tends to be accelerated by certain defect sites. When such defects tend to be present in relatively greater concentrations at the surface, the process is called **surface recombination**. In bulk crystals, the density of recombination centers can be made low for a very pure and "good" crystal. A typical recombination center concentration in a high quality Si crystal would be $\sim 10^{12}\,\text{cm}^{-3}$.

Photo-excited carriers can also be eliminated from the conduction process by **electron** and **hole traps**. These traps differ from recombination centers insofar as traps preferentially eliminate a single type of carrier. In practice, hole traps seem to be more common than electron traps. For example, in the silver halides which are important in the photographic process, the hole is trapped almost as soon as it is produced and photoconduction occurs through the electrons.

Electron and neutron irradiation of materials produce both recombination centers and traps in photoconducting materials. Thus, special precautions must be exercised in using photo-detectors in high radiation environments, such as on satellites in outer space.

Trapped electrons can be released by thermal or optical excitation. For example, consider a p-type sample of Ge which has been doped with Mn, Ni, Co, or Fe. At low temperatures E_F will be near the top of the valence band and the acceptor impurity states will have very few electrons in them. Photons that are energetic enough to take an electron from the valence band to these impurity levels will result in hole carriers in the valence bands. The deep acceptor levels for these impurities are above the top of the valence band by 0.16 eV for Mn, 0.22 eV for Ni, 0.25 eV for Co and 0.35 eV for Fe. The threshold values observed for photoconductivity in these p-type Ge samples are shown in Fig. 21.9 and the experimental results are in good agreement with this interpretation. The large increase in photoconductivity at 0.7eV corresponds to the onset of an interband transition and the threshold for this process is independent of the impurity species.

The excess carrier lifetime can be measured by using light pulses and by observing the decay in the photocurrent through measurement of the voltage across a calibrated load resistor R in the external circuit, as shown in Fig. 21.10.

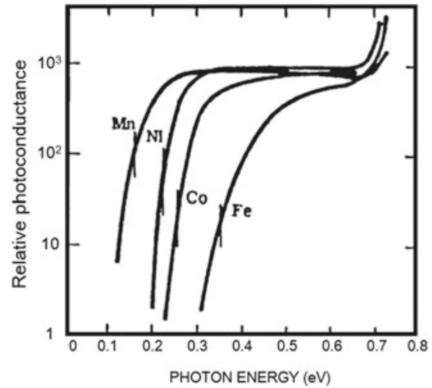

Fig. 21.9 Photoconductance spectrum occurring in the infra-red range in bulk Ge with various dopants as indicated

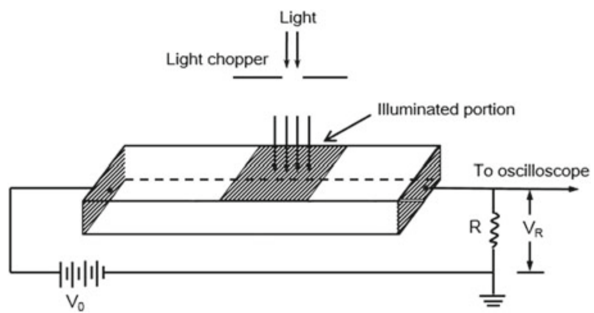

Fig. 21.10 Schematic of a circuit used to measure the excess carrier lifetime through decay in the photocurrent

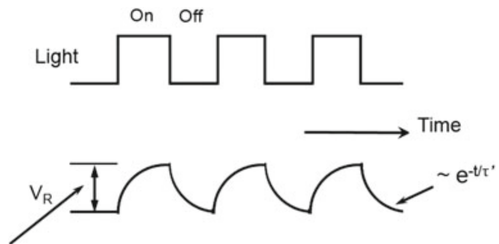

Fig. 21.11 Schematic experimental time dependence of incident light pulses and of the corresponding photoconductivity signal

For each light pulse, the carrier density will build up and then decay exponentially with a characteristic time equal to the lifetime τ' of the excess carriers generated by the light intensity coming from the photodetector signal.Using a light chopper, light pulses can be generated as indicated in Fig. 21.11.

In the interpretation of these experiments corrections must be made for surface recombination. To study a given material, the pulse repetition rate is adjusted to match approximately the excess carriers decay lifetime. For long lifetimes ($\sim 10^{-3}$ s), a mechanical chopper arrangement is appropriate. On the other hand, for short lifetimes a spark source can be used to give a light pulse of $\sim 10^{-8}$ s duration. For extremely short lifetimes, lasers with pulses well below $\sim 10^{-12}$ s are available.

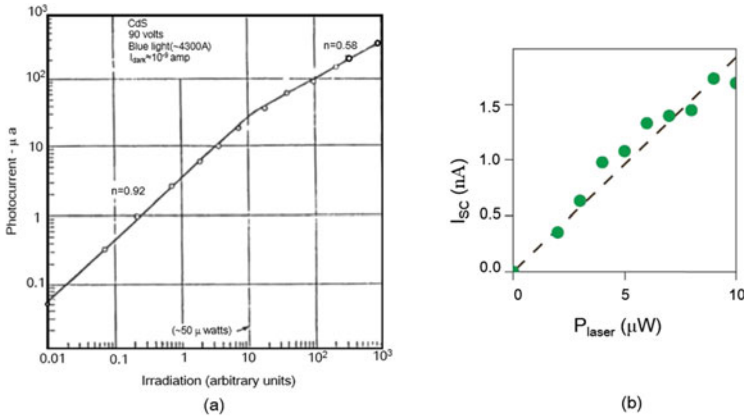

Fig. 21.12 Experimental dependence of the photocurrent on incident light irradiation for **a** CdS and **b** WSe_2. A linear response is observed for low light intensity levels. (see B.W.H. Baugher, et al. *Nature Nanotechnology*, **9**, 292, (2014).)

To get an idea of the magnitude involved in the photoconduction process, we show in Fig. 21.12 some data for CdS, a common photoconducting material used for optical devices. This plot of the photoconductive response versus illumination level shows that the photocurrent is almost a linear function of the illumination intensity for low intensities but is non-linear at high illumination levels on this log - log plot. The **dark current** refers to the background current that flows in the absence of incident light. Thus, the Fig. 21.12a shows that an incident power as small as $5\times\ 10^{-8}$ watts results in a photocurrent 50 times greater than the dark current. Figure 21.12b shows the photo-current of a WSe_2 $p-n$ junction, which exhibits a linear dependence on the incident optical power.

21.4 Photoluminescence in 2D Materials

Photoluminescence spectroscopy has become a very important tool for studying 2D layered materials including the monolayer transition metal dichalcogenides MoS_2 and WSe_2. Unlike the bulk material, monolayer MoS_2 emits light strongly, exhibiting an increase in luminescence quantum efficiency by more than a factor of 10^4 compared with the bulk material (see Mak et al. 2010). This is due to the effect of quantum confinement on the material's electronic structure, which induces an indirect-to-direct bandgap phase transition. This new family of atomically thin direct bandgap semiconductors have attracted much research interest, since direct bandgap semiconductors are more applicable to optoelectronic devices, such as LEDs, solar cells, and photodiodes. Because of the strong dependence on thickness, photoluminescence spectroscopy, together with Raman spectroscopy, is routinely used to determine the layer

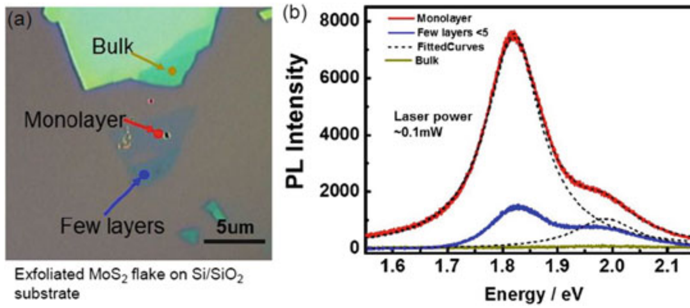

Fig. 21.13 **a** Optical microscope image and **b** photoluminescence spectra of monolayer, few-layer, and bulk MoS_2. (see Li et al. 2014)

thickness of mono- and few-layer transition metal dichalcogenides. Figure 21.13a shows an optical microscope image of MoS_2 exfoliated onto a Si/SiO_2 substrate using the conventional scotch tape method (Novoselov et al. 2004). The PL spectra of monolayer, few-layer, and bulk regions, indicated in Fig. 21.13a, are shown in Fig. 21.13b. Here, the monolayer region exhibits bright photoluminescence indicating its direct bandgap nature. The PL spectra of few layer MoS_2 shows significantly suppressed PL, and bulk MoS_2 shows almost no detectible photoluminescence.

Suggested Reading

P.Y. Yu, M. Cardona, *Fundamentals of Semiconductors* (Springer, Berlin, 1996)

References

C. Adachi, M.A. Baldo, M.E. Thompson, S.R. Forres, J. Appl. Phys. **90**, 5048–5051 (2001)
X.F. Huang, Y. Huang, R. Agarwal, C.M. Lieber, Nat. **421**, 241–245 (2003)
Z. Li, S.W. Chang, C.C. Chen, S.B. Cronin, Nano Res. **7**, 973–980 (2014)
K.F. Mak, C. Lee, J. Hone, J. Shan, T.F. Heinz, Atomically thin MoS_2: A new direct-gap semiconductor. Phys. Rev. Lett. **105**, 136805 (2010)
K.S. Novoselov et al., Electric field effect in atomically thin carbon films. Sci. **306**, 666 (2004)